Author/s:
Krishnamurthy, B;Chee, J;Jhala, G;Fynch, S;Graham, KL;Santamaria, P;Morahan, G;Allison, J;Izon, D;Thomas, HE;Kay, TWH

Title:
Complete diabetes protection despite delayed thymic tolerance in NOD8.3 TCR transgenic mice due to antigen-induced extrathymic deletion of T cells

Date:
2012-02-01

Citation:
Krishnamurthy, B., Chee, J., Jhala, G., Fynch, S., Graham, K. L., Santamaria, P., Morahan, G., Allison, J., Izon, D., Thomas, H. E. & Kay, T. W. H. (2012). Complete diabetes protection despite delayed thymic tolerance in NOD8.3 TCR transgenic mice due to antigen-induced extrathymic deletion of T cells. Diabetes, 61 (2), pp.425-435. https://doi.org/10.2337/db11-0948.

Persistent Link:
https://hdl.handle.net/11343/264790

Complete Diabetes Protection Despite Delayed Thymic Tolerance in NOD8.3 TCR Transgenic Mice Due to Antigen-Induced Extrathymic Deletion of T Cells

Balasubramanian Krishnamurthy,[1] Jonathan Chee,[1] Gaurang Jhala,[1] Stacey Fynch,[1] Kate L. Graham,[1] Pere Santamaria,[2] Grant Morahan,[3] Janette Allison,[1] David Izon,[1] Helen E. Thomas,[1,4] and Thomas W.H. Kay[1,4]

Prevention of autoimmunity requires the elimination of self-reactive T cells during their development in the thymus and maturation in the periphery. Transgenic NOD mice that overexpress islet-specific glucose 6 phosphatase catalytic subunit–related protein (IGRP) in antigen-presenting cells (NOD-IGRP mice) have no IGRP-specific T cells. To study the relative contribution of central and peripheral tolerance mechanisms to deletion of antigen-specific T cells, we crossed NOD-IGRP mice to highly diabetogenic $IGRP_{206–214}$ T-cell receptor transgenic mice (NOD8.3 mice) and studied the frequency and function of IGRP-specific T cells in the thymus and periphery. Peripheral tolerance was extremely efficient and completely protected NOD-IGRP/NOD8.3 mice from diabetes. Peripheral tolerance was characterized by activation of T cells in peripheral lymphoid tissue where IGRP was expressed followed by activation-induced cell death. Thymectomy showed that thymic output of IGRP-specific transgenic T cells compensated for peripheral deletion to maintain peripheral T-cell numbers. Central tolerance was undetectable until 10 weeks and complete by 15 weeks. These in vivo data indicate that peripheral tolerance alone can protect NOD8.3 mice from autoimmune diabetes and that profound changes in T-cell repertoire can follow subtle changes in thymic antigen presentation. ***Diabetes*** **61:425–435, 2012**

By exposing developing thymocytes to self-antigens, the thymus purges the majority of autoreactive T cells by a process called negative selection. Experiments in animal models have demonstrated that stromal medullary thymic epithelial cells (ECs) and bone marrow–derived thymic dendritic cells (DCs) play an important role by expressing self-antigens to mediate thymocyte negative selection (1). Many, but not all, tissue-specific antigens that are expressed in medullary thymic ECs are controlled by the autoimmune regulator (AIRE) transcription factor (2–5). Thymic DCs have been shown to broaden the spectrum of self-antigens presented to developing T cells either by expressing self-antigens or presenting self-antigens after capturing them from medullary ECs (6).

Although the expression of self-antigens in medullary thymic ECs and thymic DCs deletes the majority of self-reactive T cells, the central negative selection process is still not complete. This is indicated by the presence of circulating self-reactive effector T cells in healthy individuals (7–10). For the T cells specific for self-antigens that escape central tolerance, additional protection is provided by peripheral tolerance mechanisms. In peripheral tissue, steady-state DCs and AIRE-expressing ECs make an important contribution to the inactivation/deletion of self-reactive T cells (11–15). Despite the crucial role of T-cell deletion in limiting autoimmune attack, the relative central and peripheral contributions to self-reactive T-cell tolerance to individual self-antigens are not well documented.

In humans with type 1 diabetes and in the NOD mouse, self-reactive T cells escape negative selection in the thymus, emigrate to the periphery, and are activated to differentiate into diabetogenic effector T cells. Thus, autoimmune diseases such as type 1 diabetes represent a failure of both central and peripheral tolerance mechanisms. In the NOD mouse, pathogenic autoimmunity develops against β-cell antigens, including insulin and islet-specific glucose 6 phosphatase catalytic subunit–related protein (IGRP) (16–18). Mechanisms of tolerance to these two antigens are very different. Insulin is expressed in medullary thymic ECs in an AIRE-dependent manner. Physiological insulin expression in the thymus does induce tolerance, but it is insufficient to completely protect from diabetes in NOD mice. We have previously shown that increased thymic expression of insulin can completely protect from diabetes (19). In contrast, IGRP is not expressed in the thymus of NOD mice (15,20), and peripheral tolerance is the only protection from autoimmunity to IGRP. In NOD mice, $CD8^+$ T cells that target the peptide $IGRP_{206–214}$ (IGRP-specific T cells) can be tracked using $IGRP_{206–214}$ /K^d tetramer (IGRP tetramer). They can be detected in the peripheral blood and in the islets of most NOD mice (18,21).

In NOD-IGRP mice, IGRP is transgenically overexpressed in antigen-presenting cells (APCs) of the thymus and the periphery (16). However, owing to the low frequency of IGRP-specific T cells in the endogenous repertoire, only limited insight could be gained into the relative contribution of central versus peripheral tolerance mechanisms. Thus, despite the clearly established importance of central tolerance, it remains unclear how efficiently thymic negative selection removes autoreactive T cells from the repertoire. Hence, we studied the impact on IGRP-specific T cells by transgenically introducing IGRP expression

From [1]St. Vincent's Institute, Victoria, Australia; the [2]Julia McFarlane Diabetes Research Centre and Department of Microbiology and Infectious Diseases, Faculty of Medicine, University of Calgary, Calgary, Alberta, Canada; the [3]Centre for Medical Research, University of Western Australia, Perth, Australia; and the [4]Department of Medicine, University of Melbourne, St. Vincent's Hospital, Victoria, Australia.
Corresponding author: Thomas W.H. Kay, tkay@svi.edu.au.
Received 8 July 2011 and accepted 11 October 2011.
DOI: 10.2337/db11-0948
This article contains Supplementary Data online at http://diabetes.diabetesjournals.org/lookup/suppl/doi:10.2337/db11-0948/-/DC1.

in the thymus and peripheral lymphoid tissue of T-cell receptor (TCR) transgenic NOD mice with $CD8^+$ T cells specific for this disease-relevant epitope (NOD8.3 mice). Our results demonstrate central tolerance of IGRP-specific T cells is delayed and age dependent and that peripheral tolerance is extremely efficient at being able to protect completely from IGRP-specific T cell–mediated diabetes.

RESEARCH DESIGN AND METHODS

Mice. Mice were bred and maintained under specific pathogen-free conditions at the St. Vincent's Institute. NOD/Lt mice were purchased from the Walter and Eliza Hall Institute (Melbourne, Australia). NOD8.3 mice expressing TCR-αβ rearrangement of the H-$2K^d$–restricted, β-cell reactive, $CD8^+$ T-cell clone NY8.3 and NOD-IGRP mice expressing IGRP under control of a major histocompatibility complex (MHC) class II promoter (I-E-ακ) have been described previously (16,22,23). NOD8.3/CD45.2 mice were made by crossing NOD8.3 mice with NODCD45.2 congenic mice (24). Thymectomies in 5-week-old mice were done as described (25). The institutional animal ethics committee approved all experiments.

Diabetes and insulitis. Mice were monitored using Advantage II Glucose Strips (Roche, Basel, Switzerland). Mice with two blood glucose readings of >15 mmol/L on consecutive days were considered diabetic. For histological analysis, pancreata from nondiabetic mice were placed in Bouin fixative and embedded in paraffin. Serial sections (5 μm) were cut and stained with anti-insulin followed by anti–guinea pig horseradish peroxidase (Dako, Carpinteria, CA). Staining was developed with diaminobenzidine (Sigma-Aldrich, St. Louis, MO) and counterstained with hematoxylin. Islets were grouped as follows: 0 = no infiltrate; 1 = peri-islet infiltrate; 2 = intraislet infiltrate, <50% islet destruction; 3 = intraislet infiltrate, >50% islet destruction; and 4 = complete islet destruction. From each pancreas, 20–30 islets were scored. The insulitis score was calculated as follows: [(0.25 × no. islets with stage 1) + (0.5 × no. islets with stage 2) + (0.75 × no. islets with stage 3) + (no. islets with intraislet insulitis)]/total no. of islets.

Antibodies, peptides, and flow cytometry. Antibodies used were anti-CD8 (Ly2, 53–6.7), anti-CD4 (GK1.5) conjugated to phycoethrin (PE) or APC (BioLegend, San Diego, CA), anti-CD11c (HL-3), anti-CD45.2 (104), anti-Bcl-2 (3F11), anti–Sirp-α (CD172) (P84), anti-CD69 (H1.2F3), anti-CD44 (IM7), anti–γ-interferon (IFN-γ) (XMG1.2), anti-FasL (MLF3) conjugated to fluorescein isothiocyanate or PE and anti-mouse tumor necrosis factor-α (TNF-α) (MP6-XT22), anti–V-α2 (B20.1), anti–V-α3.2 (RR3–16), anti–V-α8.3 (B21.14), and anti–V-α11.1 (RR8–1) conjugated to fluorescein isothiocyanate (BD Pharmingen, San Diego, CA). Anti–PD-1 (J43) and anti-CD326 (G8.8) were obtained from eBioscience (San Diego, CA). For BrdU staining, the APC-conjugated anti-BrdU was purchased with the BrdU flow kit (BD Pharmingen). Isotype controls were PE- or APC-conjugated rat IgG1 (R3–34) (BD Pharmingen) or PE-conjugated rat IgG2b (RTK4530) (BioLegend). The peptide $IGRP_{206–214}$ (VYLKTNVFL) was purchased from Auspep (Melbourne, Australia). The thymus, spleen, inguinal lymph node, and pancreatic lymph nodes (PLNs) were prepared as single cell suspensions. Cell surface markers were stained using standard procedures. For BrdU incorporation, mice were injected intraperitoneally with 3 μg BrdU (Sigma-Aldrich) in phosphate-buffered saline 1 day prior to harvest. Intracellular staining (Cytofix Cytoperm Plus kit; BD Pharmingen), the detection of BrdU incorporation (BrdU Flow kit; BD Pharmingen), a FoxP3 staining kit (eBioscience), and an apoptosis detection kit for Annexin V staining (Sigma-Aldrich) were used following the manufacturers' protocols. The specificity of staining was confirmed using isotype control antibodies. All analysis was performed on a FACSCalibur (Becton Dickinson, Franklin Lakes, NJ) using FlowJo analysis software (Treestar, Ashland, OR).

Carboxyfluorescein succinimidyl ester labeling and adoptive transfer. $CD8^+$ T cells from NOD8.3 mice were labeled with carboxyfluorescein succinimidyl ester (CFSE) as previously described (16). For deletion experiments, mice were given 2×10^7 CFSE-labeled splenic T cells from NOD8.3 mice. Two weeks after T-cell transfer, spleen and lymph nodes were harvested from recipient NOD or NOD-IGRP mice and transferred T-cell numbers were determined by flow cytometry by analyzing $CFSE^+$ IGRP $tetramer^+$ $CD8^+$ T cells as previously described (26).

Expression analysis. Thymic stromal cells and thymic DCs were isolated from the whole thymus as previously described (27). Thymic ECs and DCs were sorted using the following markers: ECs, propidium $iodide^-$, $CD45^-$, $CD11c^-$, MHC II^+, and $CD326^+$; DCs, propidium $iodide^-$, $CD45^+$, $CD11c^+$, MHC II^+, and $CD326^-$. Total RNA was prepared from sorted thymic ECs and DCs using TRIzol reagent (Invitrogen, Carlsbad, CA). Total RNA was reverse transcribed using random primers (Promega, Madison, WI) and AMV Reverse Transcriptase (Promega). Real-time RT-PCR analysis was performed with Assay-on-Demand kits (Applied Biosystems, Carlsbad, CA) for mouse IGRP and β-actin (housekeeping gene). Analysis was performed on a Rotor-Gene-3000 (Corbett Research, Corbett Life Science, Sydney, Australia).

Thymic grafting. Thymic lobes from 1-day-old donor CD45.2 NOD or NOD8.3 mice were grafted under the kidney capsule of anesthetized 8-week-old recipient NOD or NOD-IGRP CD45.1 mice. After 2 weeks, grafted thymic lobes were recovered and processed individually. Thymic lobes were digested in collagenase/DNase and analyzed by flow cytometry.

Statistics. Analyses of data were performed using GraphPad Prism (GraphPad Prism Software, San Diego, CA), and the Mann-Whitney *U* test was used to assess statistical significance.

RESULTS

NOD-IGRP/NOD8.3 mice are completely protected from diabetes. Expression of autoantigens in the APC is a robust way to induce tolerance. NOD-IGRP mice express IGRP under the MHC class II (I-E-ακ) promoter (16). As a result, IGRP-specific T cells are not detected in the thymus, periphery, or islets of these mice. NOD-IGRP mice were crossed to NOD TCR transgenic mice that have ~90% of $CD8^+$ T cells specific for $IGRP_{206–214}$ (NOD8.3 mice) (23). We crossed NOD8.3 mice to two different founder lines of NOD-IGRP mice, and the phenotype was identical in both the resulting NOD-IGRP/NOD8.3 lines. NOD8.3 mice, as described previously, showed accelerated diabetes with >70% of the mice developing diabetes before 100 days as a result of infiltration of islets with IGRP-specific $CD8^+$ T cells. In contrast, NOD-IGRP/NOD8.3 mice developed significantly reduced insulitis and were completely protected from diabetes (Fig. 1*A*–*D*). In NOD8.3 mice, aged 40 days, ~80% of the islets were infiltrated with lymphocytes (Fig. 1*C* and *D*) and >50% of the islets were completely destroyed. In NOD-IGRP/NOD8.3 mice, even at age 100 days, only ~40% of the islets were infiltrated with lymphocytes and <10% of the islets were completely destroyed. There was no progression of destructive insulitis (scores of 3 or 4) at any stage between age 40 and 300 days (Fig. 1*D*, data shown to age 150 days only). Because the diabetic mice were excluded for insulitis scoring, NOD8.3 mice with less insulitis were selected for analysis. Hence, even though there is progression in insulitis in NOD8.3 mice, this is not reflected in the insulitis score.

Thymic selection in NOD-IGRP/NOD8.3 mice. When NOD-IGRP/NOD8.3 mice were studied up to age 60–70 days, there was no evidence of central deletion. Young NOD-IGRP/NOD8.3 mice displayed thymic CD8-to-CD4 ratios similar to NOD8.3 mice (Fig. 2*A* and Supplementary Fig. 1*A*). This suggests that positive selection of NOD8.3 T cells occurs normally both in the absence of thymic IGRP expression in NOD8.3 mice (20) and in its presence in NOD-IGRP/NOD8.3 mice. The proportion of $CD8^+$ thymocytes that bound IGRP tetramer and the intensity of tetramer binding was similar in NOD8.3 and NOD-IGRP/NOD8.3 mice (Fig. 2*A*, *middle*). The absolute number of $CD8^+$ thymocytes was similar in young NOD8.3 and NOD-IGRP/NOD8.3 mice (Supplementary Fig. 1*A*). We questioned if thymocytes escaped central tolerance by expressing lower surface levels of the IGRP-specific TCR together with an alternate TCR (transgenic V-β and endogenous V-α). However, when we crossed NOD-IGRP/NOD8.3 on to the $Rag1^{-/-}$ background to prevent cells expressing a second receptor, the lack of deletion was unchanged (Fig. 2*B* and Supplementary Fig. 1*E*), indicating this was not the case. Moreover, the intensity of IGRP tetramer binding in young NOD-IGRP/NOD8.3 was similar to NOD8.3 thymocytes (Fig. 2*A* and *B*). Thus, we concluded that NOD8.3 T cells were not deleted in the thymus possibly because of insufficient IGRP expression.

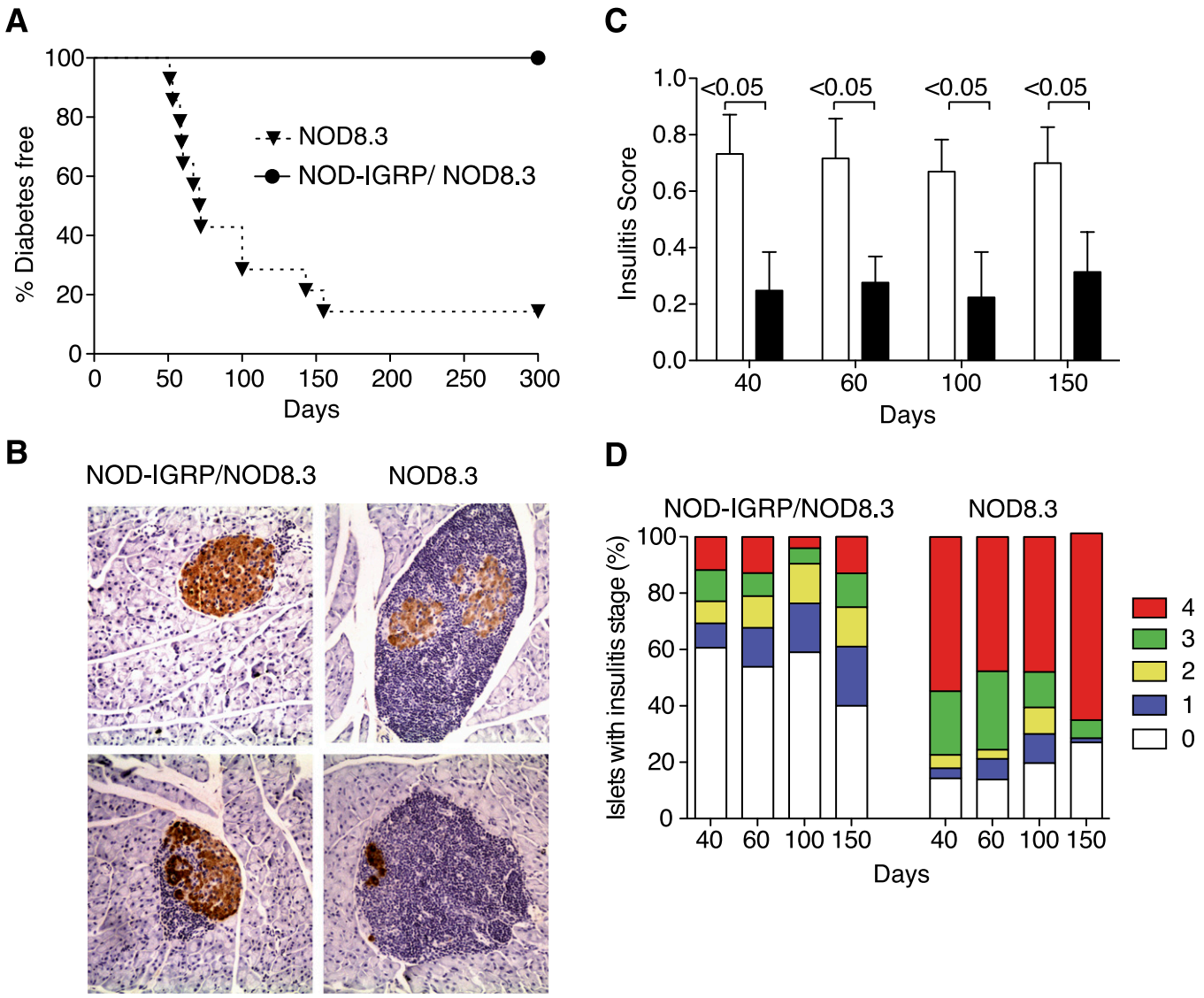

FIG. 1. NOD-IGRP/NOD8.3 mice are protected from diabetes and have less severe insulitis. *A*: Incidence of diabetes in NOD8.3 (n = 20) and NOD-IGRP/NOD8.3 (n = 20) mice, $P < 0.0001$. *B*: Pancreata from 60-day-old NOD-IGRP/NOD8.3 and NOD8.3 mice were fixed and embedded in paraffin. Sections were stained with anti-insulin antibody and counterstained with hematoxylin. Representative sections are shown. *C*: More than 100 pancreatic islets from NOD-IGRP/NOD8.3 (black bar) and NOD8.3 (white bar) mice were evaluated for lymphocytic infiltration at age 40, 60, 100, and 150 days (n = 5 mice per strain per age-group). The y-axis represents the mean ± SD of the insulitis score. *D*: Insulitis stages at age 40, 60, 100, and 150 days (n = 5 mice per strain per age-group). (A high-quality digital representation of this figure is available in the online issue.)

Systemic activation of IGRP-specific T cells in NOD-IGRP/NOD8.3 mice does not trigger cytotoxic T-lymphocyte differentiation. Without evidence of central tolerance, we expected robust peripheral tolerance to explain the complete protection from diabetes in NOD-IGRP/NOD8.3 mice. We tested the fate of IGRP-specific T cells in the peripheral lymphoid organs. The phenotype of T cells from draining PLNs, nondraining inguinal lymph nodes, and spleen were similar in NOD-IGRP/NOD8.3 (data not shown). Analogous to what is seen in thymocytes, IGRP-specific T cells from peripheral lymphoid organs of young NOD-IGRP/NOD8.3 mice displayed CD8-to-CD4 ratios similar to NOD8.3 mice (Fig. 3*A* and Supplementary Fig. 1*B*, spleen data shown). However, in contrast to thymocytes, IGRP-specific T cells in the peripheral lymphoid organs of young NOD-IGRP/NOD8.3 mice underwent activation and proliferation in the periphery. IGRP-specific T cells in NOD-IGRP/NOD8.3 mice displayed an activated phenotype because they expressed significantly more CD69, CD44, and PD-1 and incorporated more BrdU, indicating increased proliferation (Fig. 3*B*). The $CD8^+$ T cells of NOD-IGRP/NOD8.3 mice showed an additional CD8 low population, suggesting activation-induced down-regulation of the TCR (Fig. 3*A*, *top*). In addition, even though most $CD8^+$ splenocytes from NOD-IGRP/NOD8.3 mice bound IGRP tetramers, the intensity of tetramer binding was significantly less than in NOD8.3 mice (Fig. 3*A*, *bottom*), consistent with activation. The mean fluorescence intensity of IGRP $tetramer^+$ $CD8^+$ T cells in young NOD-IGRP/NOD8.3 compared with NOD8.3 mice was 711 ± 37 vs. 1071 ± 38 (P = 0.0001). It was surprising that NOD-IGRP/NOD8.3 mice were protected from diabetes when IGRP-specific T cells underwent activation and proliferation after encountering antigen in the periphery.

As thymic expression of self-antigens can induce antigen-specific regulatory T cells, we analyzed if the protection

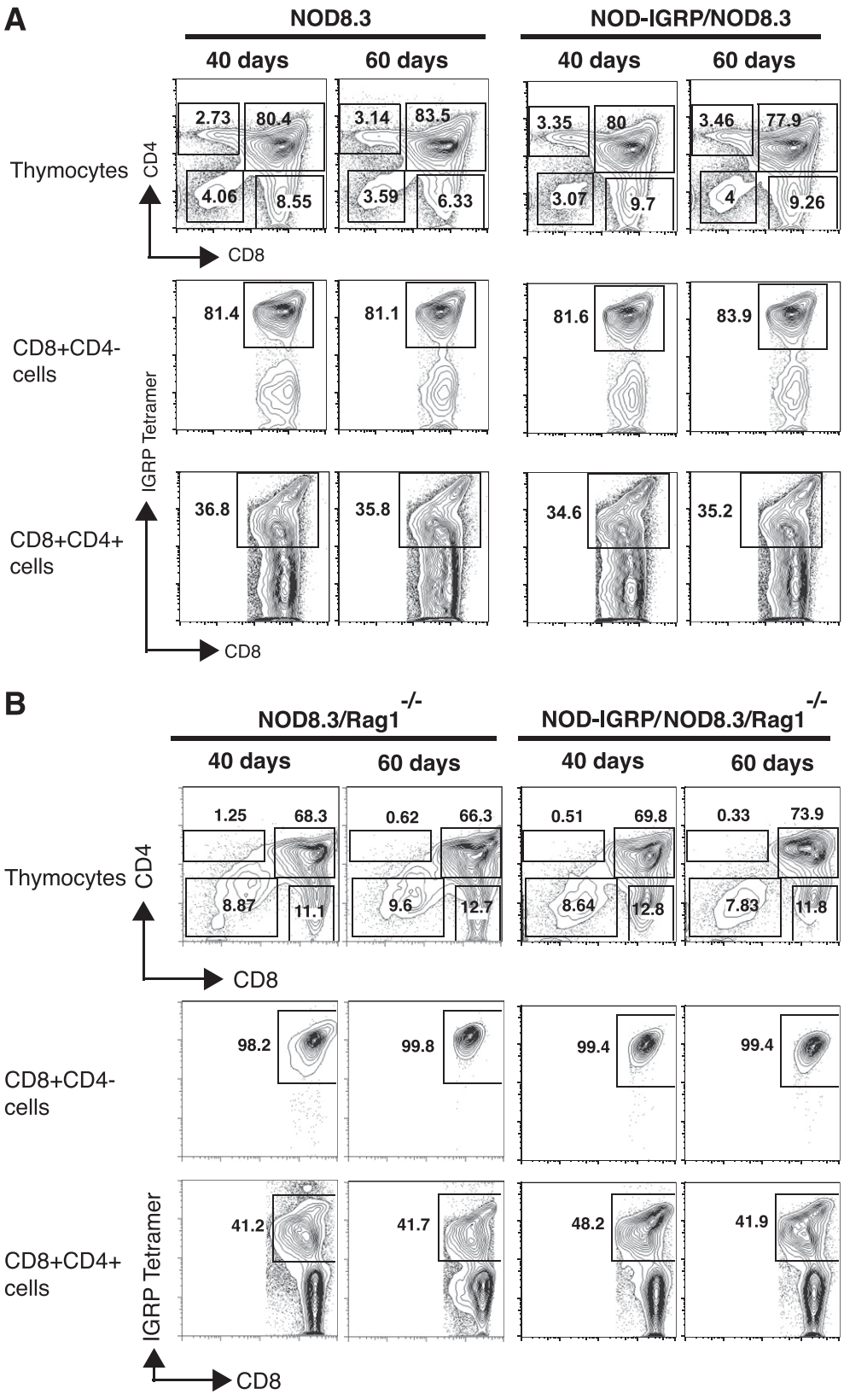

FIG. 2. IGRP-specific T cells are not deleted in the thymus of young NOD-IGRP/NOD8.3 mice. *A*: Representative CD4 versus CD8 plots of cell suspensions from thymus of NOD8.3 and NOD-IGRP/NOD8.3 mice (*top*). IGRP tetramer$^+$ CD8$^+$ T cells after gating on the CD8 single-positive subset (*middle*) or CD8$^+$CD4$^+$ double-positive subset (*bottom*). Numbers indicate the percentage of live cells (*top*) or the percentage of tetramer$^+$ cells in the CD8$^+$ subset (*middle*) or CD8$^+$CD4$^+$ double-positive subset (*bottom*); *n* = 6–9 mice per strain per age-group. Pooled data are shown in Supplementary Fig. 1*A*. *B*: Representative CD4 versus CD8 plots of cell suspensions from thymus of NOD8.3/Rag1$^{-/-}$ and NOD-IGRP/NOD8.3/Rag1$^{-/-}$ mice (*top*). IGRP tetramer$^+$ CD8$^+$ T cells after gating on CD8 single-positive (*middle*) and CD8$^+$CD4$^+$ double-positive subsets (*bottom*). Numbers indicate the percentage of live cells (*top*) or the percentage of tetramer$^+$ cells in CD8$^+$ subsets (*middle*) or CD8$^+$CD4$^+$ double-positive subsets (*bottom*); *n* = 4–6 mice per strain per age-group. Pooled data are shown in Supplementary Fig. 1*E*.

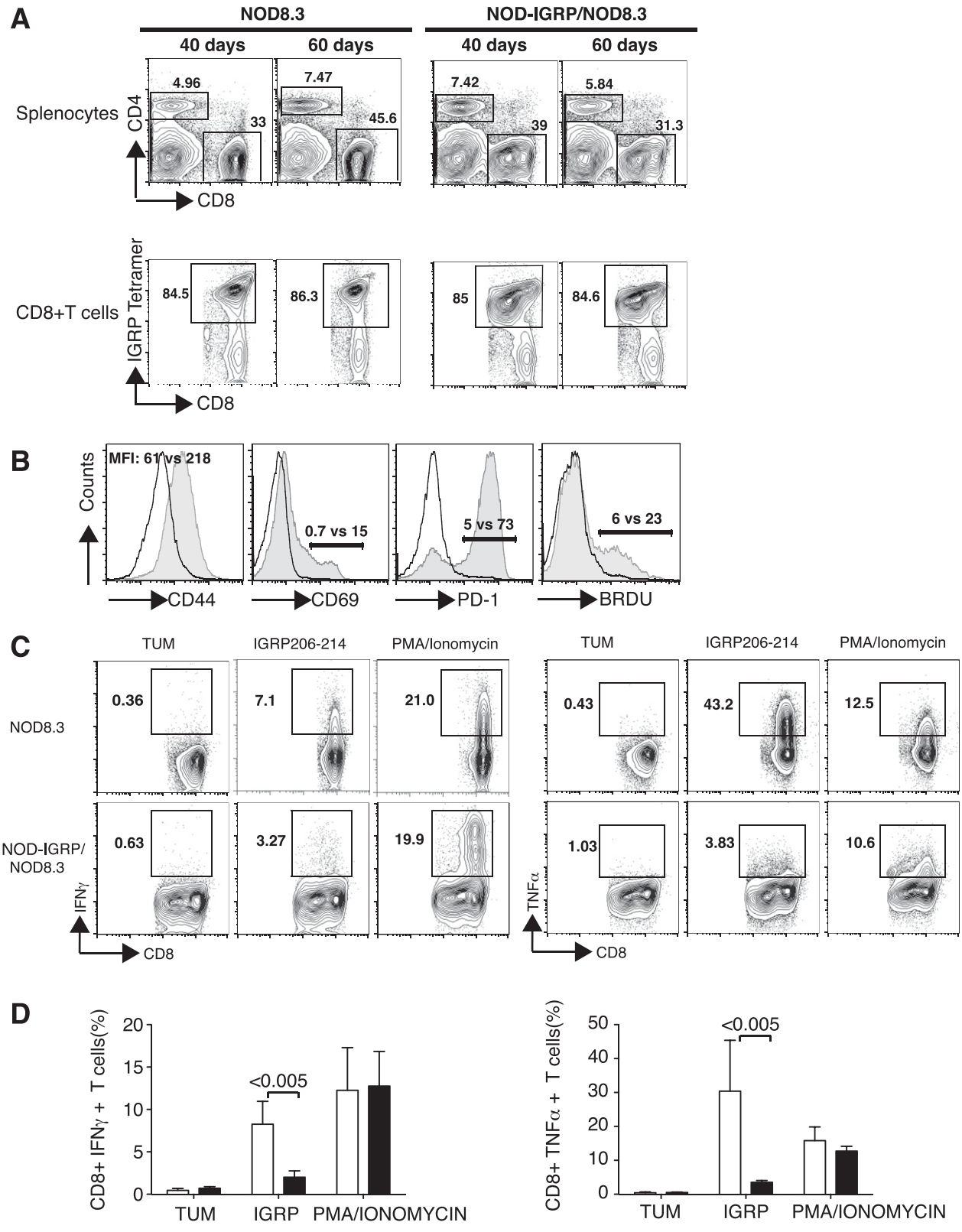

FIG. 3. IGRP-specific CD8+ T cells in young NOD-IGRP/NOD8.3 mice undergo activation, proliferation, and then deletion in the periphery. *A*: Representative CD4 versus CD8 plots of cell suspensions from spleen of NOD8.3 mice and NOD-IGRP/NOD8.3 (*top*). IGRP tetramer$^+$ CD8$^+$ T cells after gating on CD8 subset (*bottom*). Numbers indicate the percentage of live cells (*top*) or the percentage of tetramer$^+$ cells in CD8 subset (*bottom*); n = 6–9 mice per strain per age-group. Pooled data are shown in Supplementary Fig. 1*B*. *B*: Representative histograms showing staining of IGRP tetramer$^+$ CD8$^+$ T cells for indicated markers. NOD8.3 profiles (white) superimposed on the profiles for NOD-IGRP/NOD8.3 mice (gray). Values on the panels for CD44 staining represent the mean fluorescence intensity (MFI). Values on all other panels correspond to percentage of cells contained within the gate; n = 3–5 mice (aged 40–60 days) per group. *C*: Representative plots of intracellular IFN-γ or TNF-α staining of CD8$^+$ splenocytes from NOD8.3 or NOD-IGRP/NOD8.3 mice (aged 40–60 days) after stimulation for 5 h with 0.1 μmol/L of IGRP$_{206–214}$ peptide, irrelevant transplantation antigen P198 (TUM) peptide, or phorbol myristic acid (PMA; 10 ng/mL) plus ionomycin (250 ng/mL). *D*: Bar graph showing the percentage of CD8$^+$ T cells secreting IFN-γ or TNF-α in NOD8.3 (white) and NOD-IGRP/NOD8.3 (black) mice after stimulation. Error bars indicate SD; n = 4–8 mice per strain (*C*) and (*D*).

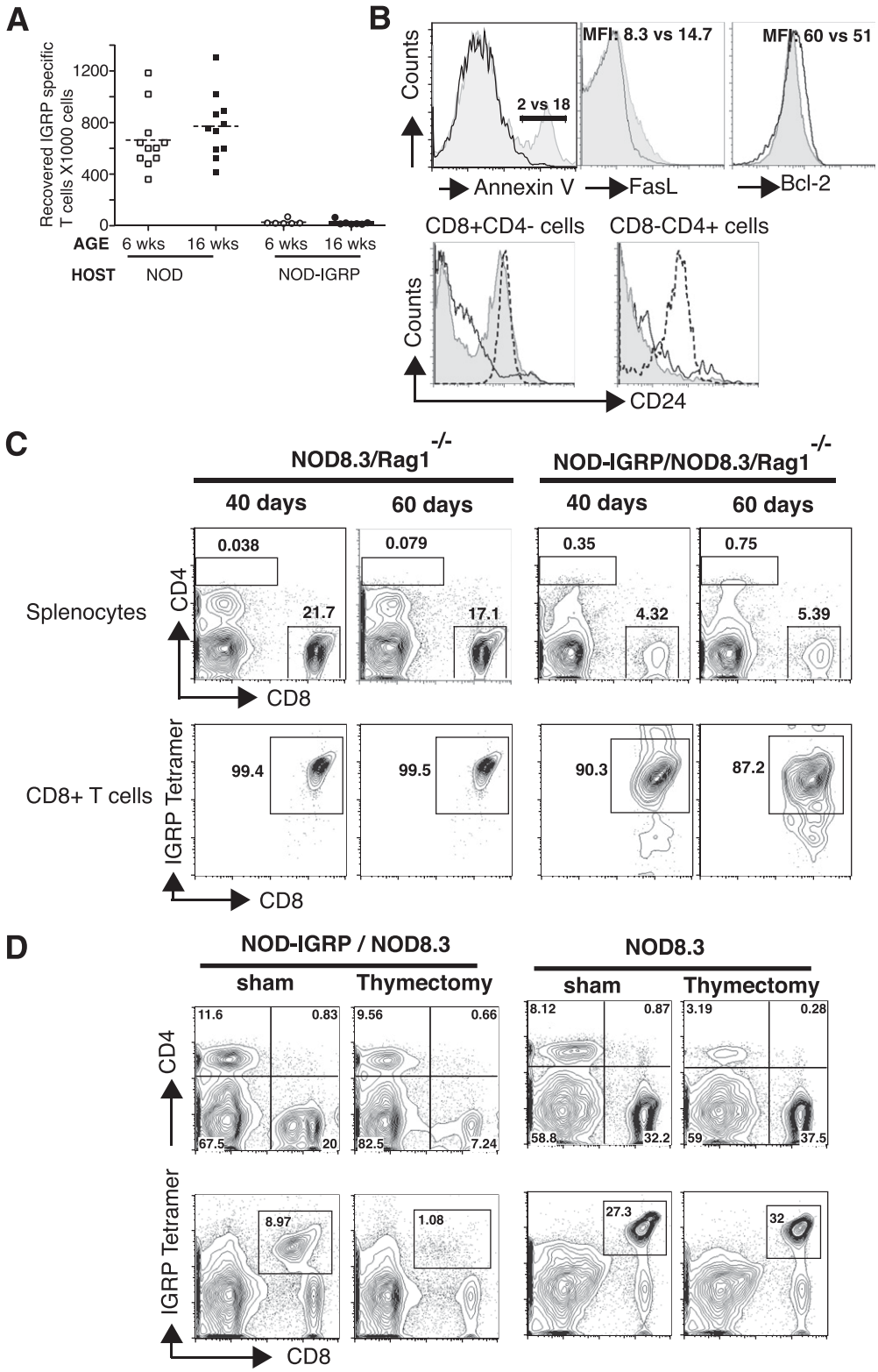

FIG. 4. Efficient peripheral deletion of IGRP-specific T cells in NOD-IGRP/NOD8.3 mice. *A*: NOD or NOD-IGRP mice were injected intravenously with 2×10^7 CFSE-labeled splenic T cells from NOD8.3 mice. Two weeks after injection, the number of CFSE$^+$ CD8$^+$ tetramer$^+$ cells remaining in the spleen and lymph nodes of the mice was determined by flow cytometry. Pooled data are shown from three independent experiments, and mean is indicated by the dashed line. *B*: Representative histograms showing staining of splenic IGRP tetramer$^+$ CD8$^+$ T cells for Annexin V, CD8$^+$ T cells for FasL, CD8$^+$ T cells for Bcl-2, and CD8$^+$ or CD4$^+$ T cells for CD24. NOD8.3 profiles (white) superimposed on the profiles for NOD-IGRP/NOD8.3 mice (gray). In the histogram showing CD24 expression, as a positive control for CD24 expression, the level of CD24 expression on respective CD8 or CD4 single-positive thymocytes is represented by the dashed black line. Values on the panel correspond to percentage of cells contained within the gate for Annexin V and the mean fluorescence intensity (MFI) for FasL and Bcl-2 staining; *n* = 3–5 mice (aged 40–60 days) per group. *C*: Representative CD4 versus CD8 plots of cell suspensions from spleen of NOD8.3/Rag1$^{-/-}$ and NOD-IGRP/NOD8.3/Rag1$^{-/-}$ mice (*top*). IGRP tetramer$^+$ CD8$^+$ T cells after gating on CD8$^+$ T cells (*bottom*). Numbers indicate the percentage of live cells (*top*) or the percentage of tetramer$^+$ cells in CD8$^+$ T cells (*bottom*); *n* = 4–6 mice per strain per age-group. Pooled data are shown in Supplementary Fig. 1*F*. *D*: NOD-IGRP/NOD8.3 or NOD8.3 mice (aged 5 weeks) were thymectomized or sham thymectomized and splenic IGRP-specific T cells were analyzed 3 weeks later; *n* = 4 mice per strain per group.

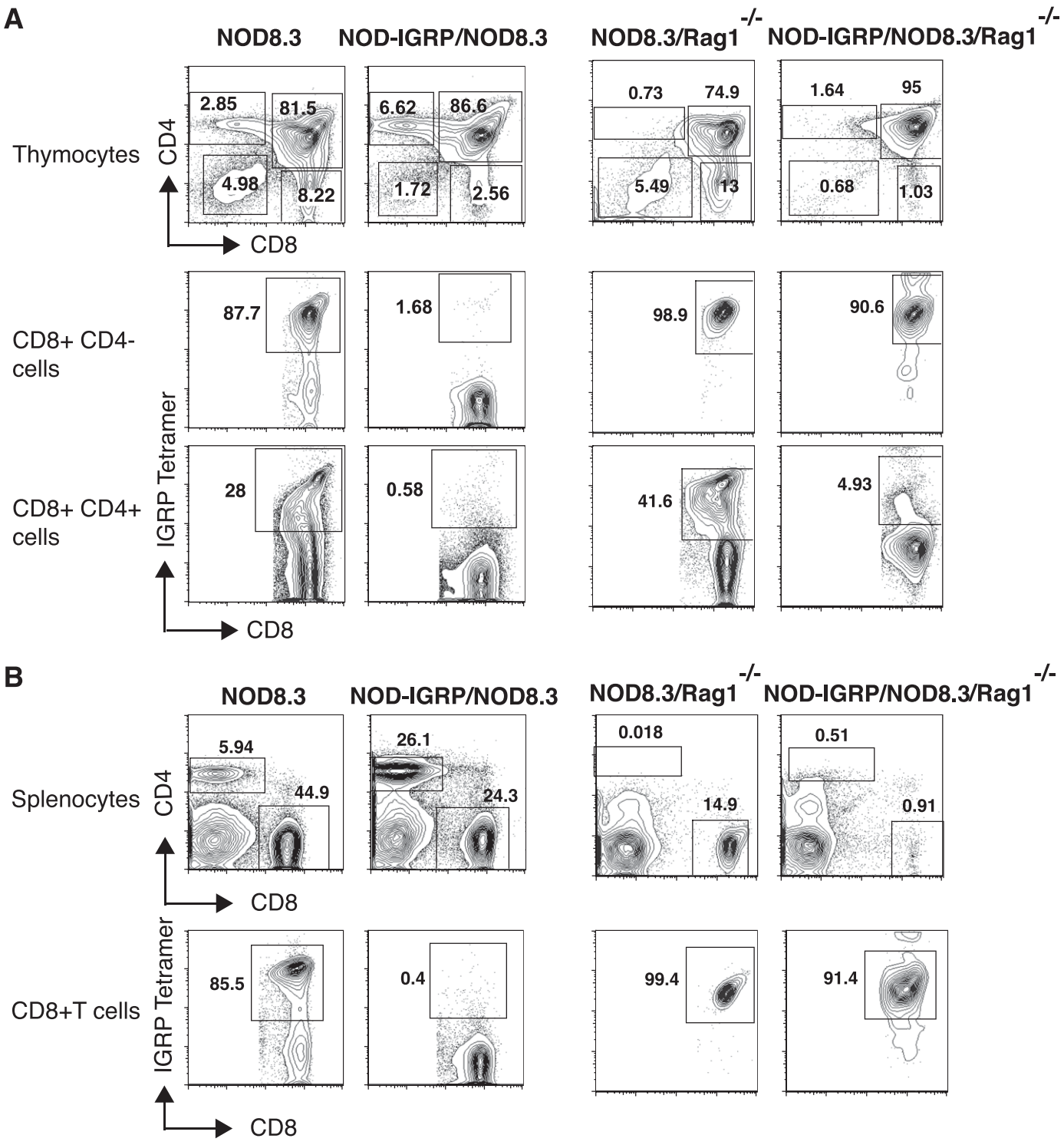

FIG. 5. Age-dependent thymic tolerance of IGRP-specific CD8$^+$ T cells in NOD-IGRP/NOD8.3 mice. *A*: Representative CD4 versus CD8 plots of cell suspensions from thymus of 100-day-old NOD8.3, NOD-IGRP/NOD8.3, NOD8.3/Rag1$^{-/-}$, and NOD-IGRP/NOD8.3/Rag1$^{-/-}$ mice (*top*). IGRP tetramer$^+$ CD8$^+$ T cells after gating on the CD8 single-positive subset (*middle*) or CD8$^+$CD4$^+$ double-positive subset (*bottom*). Numbers indicate the percentage of live cells (*top*) or the percentage of tetramer$^+$ cells in the CD8$^+$ subset (*middle*) or CD8$^+$CD4$^+$ double-positive subset (*bottom*). NOD8.3 and NOD-IGRP/NOD8.3 plots (n = 6–9 mice per strain); NOD8.3/Rag1$^{-/-}$ and NOD-IGRP/NOD8.3/Rag1$^{-/-}$ plots (n = 4–6 mice per strain). Pooled data are shown in Supplementary Fig. 1*C* and *G*. *B*: Representative CD4 versus CD8 plots of cell suspensions from spleen of 100-day-old NOD8.3, NOD-IGRP/NOD8.3, NOD8.3/Rag1$^{-/-}$, and NOD-IGRP/NOD8.3/Rag1$^{-/-}$ mice (*top*). IGRP tetramer$^+$ CD8$^+$ T cells after gating on CD8 subset (*bottom*). Numbers indicate the percentage of live cells (*top*) or the percentage of tetramer$^+$ cells in CD8 subset (*bottom*). NOD8.3 and NOD-IGRP/NOD8.3 plots (n = 6–9 mice per strain); NOD8.3/Rag1$^{-/-}$ and NOD-IGRP/NOD8.3/Rag1$^{-/-}$ plots (n = 4–6 mice per strain). Pooled data are shown in Supplementary Fig. 1*D* and *H*.

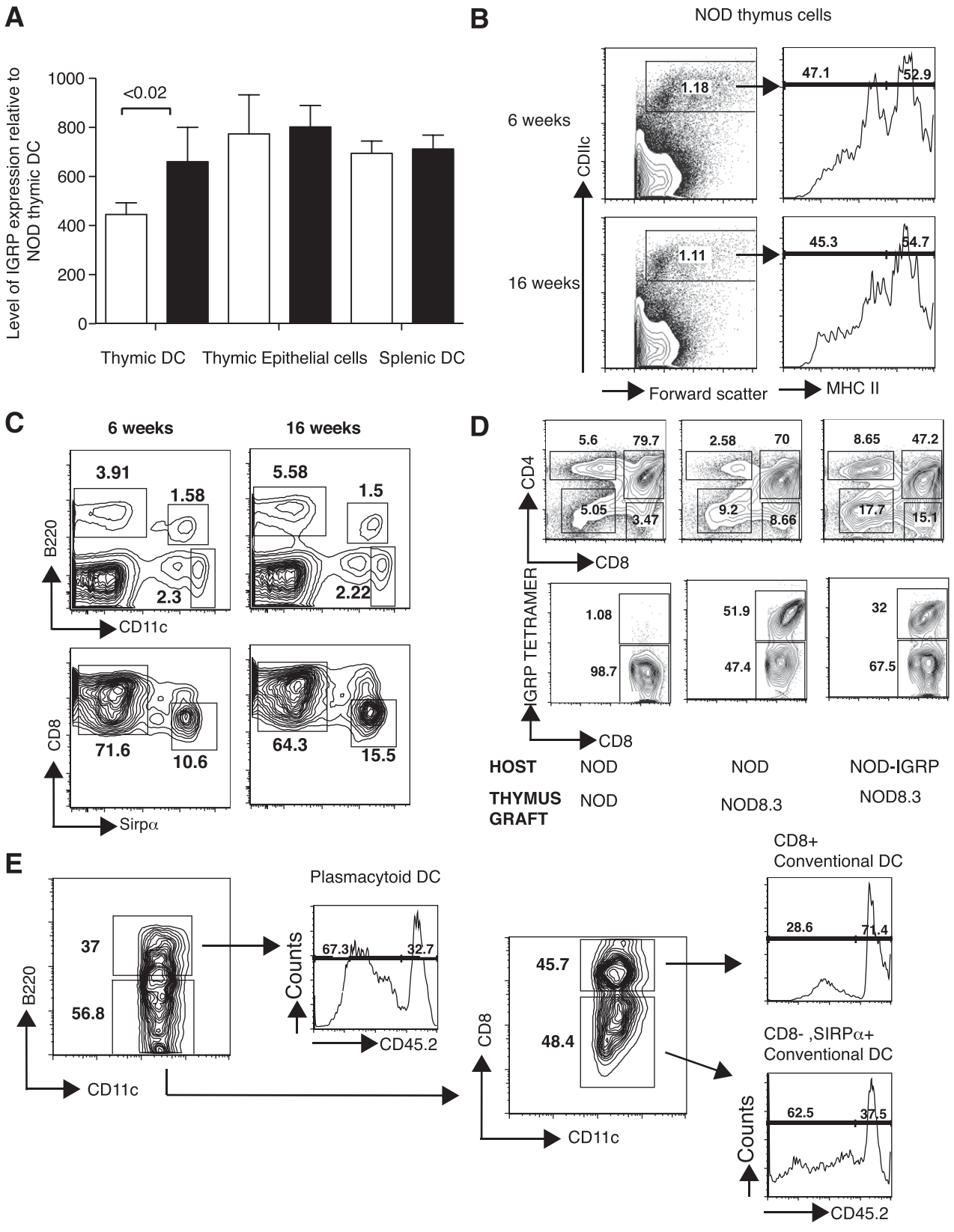

FIG. 6. Plasmacytoid and Sirp-α$^+$ DCs can migrate from periphery into the thymus and mediate IGRP-specific T cell deletion. *A*: Expression of transgenic IGRP mRNA in thymic DCs and thymic stromal ECs of 6- and 16-week-old NOD-IGRP mice (white and black bar, respectively). Total RNA from 6- and 16-week-old NOD-IGRP mice (pooled data from three independent experiments, *n* = 12 in each group) was reverse transcribed using random primers. Real-time RT-PCR was performed with Assay-on-Demand kits for mouse IGRP and β-actin. Error bars indicate SD. *B*: Thymuses (*n* = 4 in each group) from 6- and 16-week-old female NOD mice were pooled and analyzed by first gating on live cells and then analyzed for the proportion of CD11c-expressing DCs and further analyzed for the level of expression of MHC class II by the thymic DCs. *C*: Thymuses (*n* = 4 in each group) from 6- and 16-week-old female NOD mice were pooled, and the enriched thymic DCs were analyzed for the proportion of various subsets of DCs. Data shown are representative of two experiments. *D* and *E*: Thymic lobes from CD45.2 NOD or NOD8.3 mice were grafted under the kidney capsule of

from diabetes was due to an increase in regulatory T cells. However, there was no increase in FoxP3-expressing regulatory T cells in the periphery of NOD-IGRP/NOD8.3 mice compared with NOD8.3 mice (Supplementary Fig. 2*A*). In NOD-IGRP/NOD8.3 mice, the IGRP-specific T cells encounter antigen in the periphery in a noninflammatory context, and the proliferation might not lead to generation of effector T cells. After in vitro stimulation with IGRP peptide, IGRP-specific T cells from NOD-IGRP/NOD8.3 mice secreted significantly less IFN-γ and TNF-α compared with NOD8.3 mice (Fig. 3*C* and *D*). There was no difference in IFN-γ and TNF-α secretion between IGRP-specific T cells from NOD-IGRP/NOD8.3 mice and NOD8.3 mice after nonspecific phorbol myristic acid/ionomycin stimulation (Fig. 3*C* and *D* and Supplementary Fig. 2*B*). Furthermore, the absolute number and proportion of $CD8^+$ T cells in NOD8.3 mice increased with age, but this increase was not observed in NOD-IGRP/NOD8.3 mice, suggesting that IGRP-specific T cells were being deleted in the periphery (Fig. 3*A* and Supplementary Fig. 1*B*, *middle*). These data indicate that complete protection from diabetes in NOD-IGRP/NOD8.3 mice is due to ongoing peripheral tolerance from a young age.

IGRP-specific T cells from NOD-IGRP/NOD8.3 mice undergo peripheral tolerance in young mice. To address the efficiency of peripheral tolerance, we transferred CFSE-labeled IGRP-specific T cells from NOD8.3 mice into 6- or 16-week-old NOD or NOD-IGRP host mice. Three days after transfer, labeled T cells underwent extensive proliferation in NOD-IGRP mice in spleen and lymph nodes, whereas the cells proliferated only in PLN of NOD mice (data not shown) (16). Annexin V staining of transferred $CD8^+$ T cells showed that a significantly higher proportion of proliferating $CD8^+$ T cells underwent apoptosis in NOD-IGRP/NOD8.3 compared with NOD8.3 mice (Supplementary Fig. 2*C*). Two weeks after transfer, $CFSE^+$ IGRP $tetramer^+$ T cells were not detected in NOD-IGRP mice, whereas they were still detected in NOD mice (Fig. 4*A* and Supplementary Fig. 2*D*). There was no difference between 6- and 16-week-old hosts. These data indicate that peripheral tolerance to IGRP is efficient in young mice.

The deletion of IGRP-specific T cells was more obvious in NOD-IGRP/NOD8.3/$Rag1^{-/-}$ mice, in which we saw a reduction in the proportion of splenic IGRP-specific $CD8^+$ T cells in young (aged 40 or 60 days) mice as compared with NOD8.3 $Rag1^{-/-}$ mice (Fig. 4*C*). This is because all the peripheral T cells in these Rag-deficient mice are IGRP-specific $CD8^+$ T cells, whereas in NOD-IGRP/NOD8.3 mice, there was an increased accumulation, as the animals aged, of $CD8^+$ T cells expressing nontransgenic TCR α-chains (Supplementary Fig. 2*E*). In addition, downregulation of Bcl-2 and upregulation of FasL was noted in $CD8^+$ T cells of NOD-IGRP/NOD8.3 mice as compared with NOD8.3, indicating the $CD8^+$ T cells from NOD-IGRP/NOD8.3 mice were undergoing activation-induced cell death in the periphery (Fig. 4*B*). Moreover, Annexin V staining of $CD8^+$ T cells showed that a significantly higher proportion of IGRP $tetramer^+$ $CD8^+$ T cells in NOD-IGRP/NOD8.3 compared with NOD8.3 mice were undergoing apoptosis in the periphery (Fig. 4*B*). It has been shown that recent thymic emigrants undergo phenotypic maturation in the periphery with gradual (over 2 weeks) loss of CD24 expression (28). The $CD8^+$ T cells from NOD-IGRP/NOD8.3 mice expressed a higher level of CD24 as compared with that from NOD8.3 mice (Fig. 4*B*). These results suggested that the IGRP-specific $CD8^+$ T cells observed in young NOD-IGRP/NOD8.3 mice are recent thymic emigrants that were detectable before their deletion by peripheral IGRP-expressing APCs. We tested this by thymectomy of 6-week-old NOD-IGRP/NOD8.3 mice, analyzing splenic and peripheral lymph nodes for IGRP-specific $CD8^+$ T cells after 3 weeks. When compared with NOD-IGRP/NOD8.3 mice that underwent sham thymectomy, IGRP-specific $CD8^+$ T cells were almost completely deleted in NOD-IGRP/NOD8.3 mice after thymectomy (Fig. 4*D*, spleen data shown). Thus, maintenance of detectable IGRP-specific T cells in these mice depends on thymic output. Collectively, these data indicate that most IGRP-specific T cells respond to IGRP presented by APCs in the periphery by upregulating activation markers and proliferation, but this is followed by deletion.

IGRP-specific thymocytes undergo age-dependent central tolerance in NOD-IGRP/NOD8.3 mice. In the thymus and peripheral lymphoid organs, IGRP-specific T cells can be detected until age 100 days in NOD-IGRP/NOD8.3 and NOD-IGRP/NOD8.3/$Rag1^{-/-}$ mice, but we were surprised to find they then disappeared (Fig. 5*A* and *B* and Supplementary Fig. 1*C* and *D*). Analysis of thymocytes and splenocytes isolated from mice aged >100 days revealed a significantly lower CD8-to-CD4 ratio and a decrease in absolute number of $CD8^+$ T cells in NOD-IGRP/NOD8.3 mice compared with NOD8.3 mice (Fig. 5*A* and *B* and Supplementary Fig. 1*C* and *D*). In addition, whereas most $CD8^+$ thymocytes from young NOD-IGRP/NOD8.3 mice bound IGRP tetramers, $CD8^+$ thymocytes from older NOD-IGRP/NOD8.3 mice did not (Fig. 5*A*, *middle* and *bottom*). This suggests that IGRP-specific thymocytes initially escaped central tolerance and were deleted only in older thymuses. To test whether delayed deletion of IGRP-specific thymocytes is due to change in level of IGRP expression in the older thymus, we sorted thymic DCs and ECs from 6- and 16-week-old NOD-IGRP mice and determined the level of IGRP expression by RT-PCR. Both thymic DCs and ECs expressed IGRP. Although there was no change in the level of IGRP expression in thymic ECs, there was an increase in level of IGRP expression in thymic DCs from 16-week-old NOD-IGRP mice as compared with 6-week-old NOD-IGRP mice (Fig. 6*A*).

Next, we analyzed DCs isolated from young and old NOD thymuses. The ratio of DCs to T cells was similar, and there was no difference in MHC class II expression levels between the DCs from young and old thymuses (Fig. 6*B*). In mouse thymus, three subsets of DCs have been identified: plasmacytoid DC and two conventional DC subsets defined based on CD8-α and Sirp-α expression (29). Although there was no difference in the absolute number of Sirp-α^+ DCs ($215 \pm 54 \times 10^3$ cells vs. $198 \pm 60 \times 10^3$), the proportion of Sirp-α^+ DCs to total DCs increased in older thymuses ($14.7 \pm 1.9\%$ vs. $10.35 \pm 0.8\%$ of conventional DCs; $P = 0.07$) (Fig. 6*C*).

CD45.1 NOD-IGRP or NOD recipients. Two weeks later, the percentage of $CD45.2^+$ IGRP $tetramer^+$ $CD8^+$ T cells was calculated in NOD8.3 (or control NOD) thymic lobes grafted into CD45.1 NOD or NOD-IGRP recipients (*D*), and the proportion of different subsets of recipient-derived $CD45.2^-$ DCs in the grafted thymic lobes from NOD and NOD-IGRP mice was determined (*E*); *n* = 3 mice per group.

To determine if the increase in Sirp-α^+ DCs in older thymuses was the result of migration of peripheral DCs and also to determine the effect of Sirp-α^+ DCs on thymic T-cell selection, neonatal thymic lobes from CD45.2/NOD8.3 mice were grafted under the kidney capsule of recipient CD45.1 NOD or CD45.1 NOD-IGRP mice. The thymic graft was removed 2 weeks after transplantation, and the phenotype of the incoming CD45.1 DCs and the resident CD45.2 IGRP-specific T cells was studied.

After 2 weeks, DCs in the grafted thymic lobes were analyzed to assess the phenotype of the host-derived CD45.1 migrating DCs. We found most of the $CD8^-$ Sirp-α^+ DCs in the thymic graft were host derived, whereas the majority of $CD8^+$ DCs were local $CD45.2^+$ cells (Fig. 6*E*). When we analyzed the thymocytes, we found the number of CD45.2 IGRP-specific T cells was reduced in lobes grafted into NOD-IGRP mice compared with control NOD mice (Fig. 6*D*). These results suggest that as the mice age, Sirp-α^+ DCs from the periphery accumulate in the thymus, and a small change in the level of IGRP expression later in life, probably contributed by the antigen presentation efficiency of Sirp-α^+ DCs, dictates deletion of IGRP-specific T cells.

DISCUSSION

IGRP expression in the thymus is undetectable in NOD mice, and $CD8^+$ T cells specific for the self-antigen $IGRP_{206–214}$ escape from the thymus and become activated in the periphery. We have previously shown that IGRP-specific T cells are not detected in NOD-IGRP mice, but owing to low frequency of endogenous IGRP-specific T cells, we could not study the contribution of central and peripheral tolerance mechanisms to the absence of IGRP-specific T cells (16). In the current study, we show that in NOD-IGRP transgenic mice, peripheral tolerance is extremely efficient, because IGRP-specific T cells decreased to almost undetectable levels 2–3 weeks after thymectomy in NOD-IGRP/NOD8.3 mice, and we were unable to detect any IGRP-specific NOD8.3 T cells 2 weeks after they were transferred into NOD-IGRP mice. The efficient peripheral tolerance accounted for complete protection from diabetes in NOD-IGRP/NOD8.3 mice. Mild degrees of insulitis were observed, but $CD8^+$ T cells did not differentiate into effectors able to destroy β-cells in response to stimulation with antigen. It is surprising that central tolerance was not as efficient as peripheral tolerance. Thymocytes were efficiently deleted in the thymus only after 10 weeks. This interesting developmental switch in central tolerance has been demonstrated only once before. In a study of experimental autoimmune encephalomyelitis, bone marrow–derived DCs were reported to mediate delayed central tolerance by presenting exogenously derived myelin basic protein (30).

We believe that the impairment in central tolerance to IGRP in the young mice resulted from inadequate IGRP expression in thymic APCs. In a previous study, when IGRP was expressed transgenically under the control of the AIRE promoter in medullary ECs (15), 8.3 T cells were efficiently deleted in the thymus. It is likely that the difference in the results of these studies is because the amount of antigen expressed in thymic APCs in young mice is below the threshold for deletion. It has been shown that peripheral DCs can migrate to the thymus and present antigen to induce deletion of T cells (31,32). It is possible that Sirp-α^+ DCs are more efficient in inducing tolerance because they are phenotypically more mature than other thymic DC subsets (29). It also is possible that the age-dependent IGRP-specific thymocyte deletion may be related to NOD thymic architectural degeneration as the mice age (33). It is likely that thymic deletion in our model is due to DCs rather than thymic epithelium (Supplementary Fig. 2*F*). Whatever the mechanism is, as the mice aged, the quantitative and/or qualitative IGRP presentation to developing T cells was boosted.

Peptide ligands with strong affinity for TCRs induce negative thymic selection, and peptide ligands with weak affinity induce positive thymic selection. The selection outcomes for strong and weak peptides are relatively independent of peptide concentration. However, for peptides with intermediate/moderate affinity, there is substantial variation in selection as a function of concentration. Most of the peptide ligands involved in autoimmunity fall in the intermediate-affinity category. IGRP has been shown to be an important autoantigen in both NOD and human type 1 diabetes (18,34,35). $IGRP_{206–214}$ is an intermediate-affinity peptide recognized by $CD8^+$ T cells bearing 8.3-like TCRs (18,20). T cells specific for this peptide fall into the affinity range in which fate is sensitively determined by antigen exposure. T cells bearing intermediate-affinity 8.3-like TCRs undergo positive selection in NOD thymus (20). If IGRP expression is absent (in nontransgenic mice) or low but detectable (in NOD-IGRP mice), then 8.3 T cells may exit the thymus and recognize the slightly higher antigen concentration in the PLNs of nontransgenic NOD mice or all lymphoid tissues in NOD-IGRP mice. Efficient peripheral tolerance compensates for the impaired thymic tolerance to completely protect NOD-IGRP mice from diabetes. A small increase in IGRP expression in thymic DCs, as the NOD-IGRP/NOD8.3 mice aged, tipped the balance from positive selection to negative selection. It is interesting that in contrast to T cells bearing 8.3-like TCRs, $CD8^+$ T cells bearing TCRs that bind to IGRP with high affinity are negatively selected in NOD thymus, even though IGRP is not expressed (20).

In our study, the availability of TCR transgenic mice and MHC class I tetramers provided an opportunity to directly follow autoreactive T cells and observe very clearly how tolerance and protection from diabetes was achieved. Antigen-specific tolerance remains an ultimate goal in diabetes prevention and treatment, and our study dissects one approach to this. In summary, our data show that the fate of autoreactive T cells is determined by very small changes in antigen expression and presentation that may occur in the development of autoimmunity. Our observation that peripheral tolerance can efficiently delete the T-cell repertoire is particularly relevant because cells in the periphery may be more easily targeted to prevent type 1 diabetes or pancreas and islet graft rejection than thymic cells.

ACKNOWLEDGMENTS

B.K. received a Career Development Award from the Juvenile Diabetes Research Foundation (JDRF) and a Centres of Clinical Research Excellence Fellowship from the National Health and Medical Research Council of Australia (NHMRC). K.L.G. received a postdoctoral fellowship from the JDRF and a Skip Martin Early Career Postdoctoral Fellowship from the Australian Diabetes Society. P.S. is a Scientist of the Alberta Heritage Foundation for Medical Research and received support from the Canadian Institutes of Health Research and the JDRF. H.E.T. received

a Career Development Award from the NHMRC. T.W.H.K. received a Millennium Research Grant from Diabetes Australia, a program project grant from JDRF, and a program grant from NHMRC. St. Vincent's Institute receives support from the Operational Infrastructure Support Scheme of the Government of Victoria. The Julia McFarlane Diabetes Research Centre is supported by the Diabetes Association (Foothills).

No potential conflicts of interest relevant to this article were reported.

B.K. designed the study, researched data, contributed to discussion, and wrote the manuscript. J.C. and G.J. researched data and contributed to discussion. S.F. assisted with experiments. K.L.G. researched data, contributed to discussion, and reviewed and edited the manuscript. P.S., J.A., D.I., H.E.T., and G.M. contributed to discussion and reviewed and edited the manuscript. T.W.H.K. designed the study, contributed to discussion, and edited the manuscript. T.W.H.K. takes full responsibility for the article and its originality.

The authors thank Bill Heath, University of Melbourne, and Wu Li, Walter and Eliza Hall Institute, Melbourne, Australia, for helpful comments on the manuscript; Jie Lin, University of Melbourne, for help with tetramer production; Dr. Robyn Sutherland, Walter and Eliza Hall Institute, for NODCD45.2 congenic mice; Daniela Novembre and Hannah Abidin, St. Vincent's Institute, Victoria, Australia, for excellent animal care; and Rochelle Ayala-Perez and Caroline Dobrzelak, St. Vincent's Institute, for genotyping.

REFERENCES

1. Klein L, Hinterberger M, Wirnsberger G, Kyewski B. Antigen presentation in the thymus for positive selection and central tolerance induction. Nat Rev Immunol 2009;9:833–844
2. Anderson MS, Venanzi ES, Klein L, et al. Projection of an immunological self shadow within the thymus by the aire protein. Science 2002;298:1395–1401
3. Liston A, Lesage S, Wilson J, Peltonen L, Goodnow CC. Aire regulates negative selection of organ-specific T cells. Nat Immunol 2003;4:350–354
4. Liston A, Gray DH, Lesage S, et al. Gene dosage—limiting role of Aire in thymic expression, clonal deletion, and organ-specific autoimmunity. J Exp Med 2004;200:1015–1026
5. Derbinski J, Gäbler J, Brors B, et al. Promiscuous gene expression in thymic epithelial cells is regulated at multiple levels. J Exp Med 2005;202:33–45
6. Gallegos AM, Bevan MJ. Central tolerance: good but imperfect. Immunol Rev 2006;209:290–296
7. Kanagawa O, Martin SM, Vaupel BA, Carrasco-Marin E, Unanue ER. Autoreactivity of T cells from nonobese diabetic mice: an I-Ag7-dependent reaction. Proc Natl Acad Sci U S A 1998;95:1721–1724
8. Ridgway WM, Fasso M, Fathman CG. A new look at MHC and autoimmune disease. Science 1999;284:749, 751
9. Lesage S, Hartley SB, Akkaraju S, Wilson J, Townsend M, Goodnow CC. Failure to censor forbidden clones of CD4 T cells in autoimmune diabetes. J Exp Med 2002;196:1175–1188
10. Kishimoto H, Sprent J. A defect in central tolerance in NOD mice. Nat Immunol 2001;2:1025–1031
11. Luckashenak N, Schroeder S, Endt K, et al. Constitutive crosspresentation of tissue antigens by dendritic cells controls CD8+ T cell tolerance in vivo. Immunity 2008;28:521–532
12. Hawiger D, Inaba K, Dorsett Y, et al. Dendritic cells induce peripheral T cell unresponsiveness under steady state conditions in vivo. J Exp Med 2001;194:769–779
13. Lee JW, Epardaud M, Sun J, et al. Peripheral antigen display by lymph node stroma promotes T cell tolerance to intestinal self. Nat Immunol 2007;8:181–190
14. Poliani PL, Kisand K, Marrella V, et al. Human peripheral lymphoid tissues contain autoimmune regulator-expressing dendritic cells. Am J Pathol 2010;176:1104–1112
15. Gardner JM, Devoss JJ, Friedman RS, et al. Deletional tolerance mediated by extrathymic Aire-expressing cells. Science 2008;321:843–847
16. Krishnamurthy B, Dudek NL, McKenzie MD, et al. Responses against islet antigens in NOD mice are prevented by tolerance to proinsulin but not IGRP. J Clin Invest 2006;116:3258–3265
17. Nakayama M, Abiru N, Moriyama H, et al. Prime role for an insulin epitope in the development of type 1 diabetes in NOD mice. Nature 2005;435:220–223
18. Lieberman SM, Evans AM, Han B, et al. Identification of the beta cell antigen targeted by a prevalent population of pathogenic CD8+ T cells in autoimmune diabetes. Proc Natl Acad Sci U S A 2003;100:8384–8388
19. French MB, Allison J, Cram DS, et al. Transgenic expression of mouse proinsulin II prevents diabetes in nonobese diabetic mice. Diabetes 1997;46:34–39
20. Han B, Serra P, Yamanouchi J, et al. Developmental control of CD8 T cell-avidity maturation in autoimmune diabetes. J Clin Invest 2005;115:1879–1887
21. Trudeau JD, Kelly-Smith C, Verchere CB, et al. Prediction of spontaneous autoimmune diabetes in NOD mice by quantification of autoreactive T cells in peripheral blood. J Clin Invest 2003;111:217–223
22. Chong MM, Chen Y, Darwiche R, et al. Suppressor of cytokine signaling-1 overexpression protects pancreatic beta cells from CD8+ T cell-mediated autoimmune destruction. J Immunol 2004;172:5714–5721
23. Verdaguer J, Yoon JW, Anderson B, et al. Acceleration of spontaneous diabetes in TCR-beta-transgenic nonobese diabetic mice by beta-cell cytotoxic CD8+ T cells expressing identical endogenous TCR-alpha chains. J Immunol 1996;157:4726–4735
24. Steptoe RJ, Stankovic S, Lopaticki S, Jones LK, Harrison LC, Morahan G. Persistence of recipient lymphocytes in NOD mice after irradiation and bone marrow transplantation. J Autoimmun 2004;22:131–138
25. Reeves JP, Reeves PA, Chin LT. Survival surgery: removal of the spleen or thymus. Curr Protoc Immunol 2001 May;Chapter 1:Unit 1.10
26. Davey GM, Starr R, Cornish AL, et al. SOCS-1 regulates IL-15-driven homeostatic proliferation of antigen-naive CD8 T cells, limiting their autoimmune potential. J Exp Med 2005;202:1099–1108
27. Gray DH, Chidgey AP, Boyd RL. Analysis of thymic stromal cell populations using flow cytometry. J Immunol Methods 2002;260:15–28
28. Boursalian TE, Golob J, Soper DM, Cooper CJ, Fink PJ. Continued maturation of thymic emigrants in the periphery. Nat Immunol 2004;5:418–425
29. Proietto AI, van Dommelen S, Zhou P, et al. Dendritic cells in the thymus contribute to T-regulatory cell induction. Proc Natl Acad Sci U S A 2008;105:19869–19874
30. Huseby ES, Sather B, Huseby PG, Goverman J. Age-dependent T cell tolerance and autoimmunity to myelin basic protein. Immunity 2001;14:471–481
31. Li J, Park J, Foss D, Goldschneider I. Thymus-homing peripheral dendritic cells constitute two of the three major subsets of dendritic cells in the steady-state thymus. J Exp Med 2009;206:607–622
32. Bonasio R, Scimone ML, Schaerli P, Grabie N, Lichtman AH, von Andrian UH. Clonal deletion of thymocytes by circulating dendritic cells homing to the thymus. Nat Immunol 2006;7:1092–1100
33. O'Reilly LA, Healey D, Simpson E, et al. Studies on the thymus of non-obese diabetic (NOD) mice: effect of transgene expression. Immunology 1994;82:275–286
34. Jarchum I, Nichol L, Trucco M, Santamaria P, DiLorenzo TP. Identification of novel IGRP epitopes targeted in type 1 diabetes patients. Clin Immunol 2008;127:359–365
35. Mallone R, Martinuzzi E, Blancou P, et al. CD8+ T-cell responses identify beta-cell autoimmunity in human type 1 diabetes. Diabetes 2007;56:613–621